


RESEARCH ARTICLE

Cellulose blends from gel extrusion and compounding with polylactic acid

Kerstin Müller^{1,2}  | Siegfried Fürtauer² | Markus Schmid³ | Cordt Zollfrank¹

¹Chair for Biogenic Polymers, Technische Universität München, Campus Straubing for Biotechnology and Sustainability, Straubing, Germany

²Materials Development, Fraunhofer Institute for Process Engineering and Packaging IVV, Freising, Germany

³Faculty of Life Sciences, Albstadt-Sigmaringen University, Sustainable Packaging Institute SPI, Sigmaringen, Germany

Correspondence

Kerstin Müller, Materials Development, Fraunhofer Institute for Process Engineering and Packaging IVV, Giggenhauser Str. 35, 85354 Freising, Germany.

Email: kerstin.mueller@ivv.fraunhofer.de

Abstract

Cellulose, dissolved in ionic liquids (IL), can be used successfully in the processing of thermoplastics. To recover the ionic liquid while maintaining the thermoplastic properties, other spacers than IL might be introduced into the cellulose network. Such blend materials have been prepared before by solution blending as reported in the literature. In this study, the preparation and investigation of cellulose and polylactic acid (PLA) blends using an extrusion process with an ionic liquid and co-solvent for intermediate compatibilization is reported. The obtained transparent films show a homogeneous morphology without phase separation. Thermal analysis showed no separated glass transition for PLA, and FTIR showed hydrogen bonding between cellulose and PLA chains. Thermal stability of the blends with a degradation onset around 270°C lies between regenerated cellulose and pure PLA. The blend tensile strength and elongation of ~40 MPa and 1.3%, respectively, were comparable to a multi-phase composite containing twice the molecular weight of PLA. Generally, mechanical performance of the blends was strongly influenced by degradation reactions mainly caused by the ionic liquid used, as well as blend morphology. The study shows that transfer from solution to extrusion processing is generally possible to obtain novel cellulose blends.

KEYWORDS

biopolymers and renewable polymers, blends, cellulose and other wood products, extrusion, ionic liquids

1 | INTRODUCTION

The idea of using cellulose in thermoplastic processing has been an ever-present topic in material research for a century. The combination of cellulose and polylactic acid (PLA) in green composites is a current topic in this context and could replace fossil materials in various applications.¹⁻⁵ Apart from using cellulose as a filler in thermoplastic matrices, only few attempts with

regard to thermoplastic processing of cellulose as a matrix have been reported so far. In addition to dry processes using high shear and pressure,^{6,7} the plastic deformation of cellulose has been studied mainly in wet processes. Cellulose hydrogels derived from solution-precipitation process were dried and subsequently hot-pressed, both changing crystallinity and structural orientation of the cellulose.⁸ Recently, pectin, a gel-forming and non-melting polysaccharide, was

This is an open access article under the terms of the [Creative Commons Attribution](https://creativecommons.org/licenses/by/4.0/) License, which permits use, distribution and reproduction in any medium, provided the original work is properly cited.

© 2022 The Authors. *Journal of Applied Polymer Science* published by Wiley Periodicals LLC.

successfully molded by thermo-compression to semi-transparent films using the natural deep eutectic solvent or its components glycerin and choline chloride as plasticizers.⁹ Regarding wet processing of cellulose, several imidazolium-based ionic liquids (IL) proved to be efficient solvents for cellulose.¹⁰ At higher cellulose concentrations, so called ionogels have shown potential in medicine, energy storage, or electrochemistry¹¹ as well as composite materials.¹² In this context, the influence of ILs has been investigated not only for cellulose, but also for other polymer composites.¹³ Recently, cellulose films via the solution-precipitation method were produced with different contents of residual IL.¹⁴ 1-Butyl-3-methylimidazolium chloride clearly acted as a plasticizer and thermomechanical processing was possible. This study also concluded that 40% residual IL was optimum to enhance mechanical properties in terms of tensile strength and elongation.¹⁴ Due to the ecological and economic disadvantages associated with IL, the use of ILs in technical applications is still limited.^{15,16} Biodegradability and ecotoxicity can be adjusted based on the combination of cation, anion and alkyl side chain moieties.¹⁵ From a technical point of view, high viscosity¹⁷ is a critical processing factor, but can be effectively reduced by the use of co-solvents.^{18,19} In addition, IL are not always innocent solvents in terms of degradation reactions, especially when combined with cellulose at elevated temperatures.²⁰ Ionic liquids are generally several times more expensive than conventional molecular solvents, which is due to the production and especially the purification costs. Therefore, this study aims to use the IL only as an intermediate solvent to enable cellulose chain availability and introduce other polymeric spacers into the cellulose network, but is extracted from the final material. Among the blends with other synthetic polymers that have been described before,^{21–23} PLA seemed to be a good blending partner for cellulose by means of compatibility. Attempts to use IL and PLA resulted in homogeneous, transparent and soil degradable blends, either by solution blending^{21,24} or via welding of cellulose nanofibers and PLA.²⁵ To the authors' knowledge, however, there have been no production trials on a technical scale to investigate potential applications to date, as most studies with IL have been conducted on a laboratory scale with a material output of a few grams. The main objective of this work was therefore to investigate whether the manufacturing process of homogeneous PLA/cellulose blends can be transferred from solution to extrusion, as this would allow easy upscaling with a material output in the kilogram range. Another question to be answered in this study is to what extent the properties of these new blends are

comparable to the properties of state-of-the-art composites using cellulose as filler.

The study presents the following process as an innovative idea for larger scale preparation: A cellulose gel is prepared by extrusion of microcrystalline cellulose (MCC) with an IL and a co-solvent, namely 1-ethyl-3-methylimidazolium acetate (EmimAc) and dimethyl sulfoxide (DMSO). In the second step, the cellulose gels are compounded with a PLA melt without further use of a solvent. The blend can be thermoplastically molded and the solvents recovered.

2 | METHODOLOGY

2.1 | Materials

MCC Parmcel 101 from wood pulp was purchased from Gustav Parmentier (Steinfurt, Germany) with a degree of polymerization (DP) of 310.²³ PLA Luminy® LX930 was purchased from Total Corbion PLA (Gorinchem, The Netherlands). This PLA grade is amorphous based on a D-isomer content of 8%. EmimAc (purity $\geq 98\%$) and DMSO (purity $\geq 99.5\%$) were received from proionic (Raaba-Grambach, Austria) and Merck (Darmstadt, Germany). Microcrystalline cellulose and PLA were dried at 60°C and 40°C, respectively, for at least 12 h prior to processing. Ethanol (purity = 99%) and hexafluoroisopropanol (HFIP; purity $\geq 99\%$) were purchased from Staub & Co.-Silbermann GmbH (Gablingen, Germany) and abcr GmbH (Karlsruhe, Germany), respectively.

2.2 | Blend preparation

Preparation of homogeneous PLA/cellulose blends was divided into three main processing steps. Figure 1 illustrates the mechanisms and interactions of the components during the preparation process.

2.2.1 | Cellulose gel extrusion

The cellulose gel formulations were extruded using a Haake Rheocord with Rheomex PTW 16 co-rotating twin screw extruder (Thermo Fisher Scientific, Karlsruhe, Germany) with a barrel diameter of 16 mm and a length-to-diameter ratio of 25. EmimAc was used as the cellulose solvent, and DMSO was added as a co-solvent to lower the viscosity, enabling stable solvent pumping and wetting of the cellulose. The ratio between EmimAc and DMSO was set to 4:1 by volume. Liquid feeding was performed with an Ecom Alpha

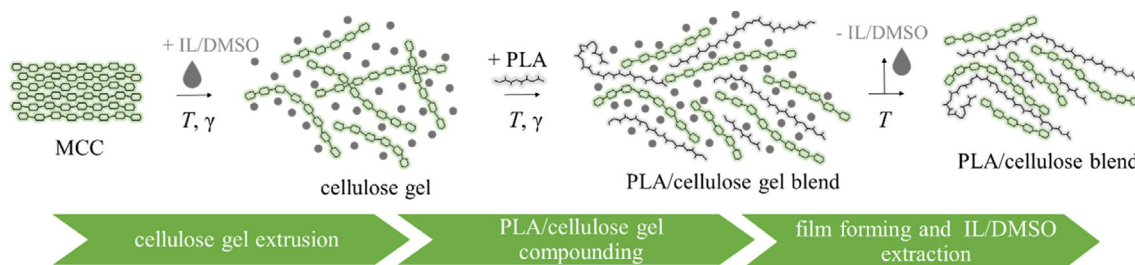


FIGURE 1 Schematic of the blend formation divided in three processing steps and the respective intermediates [Color figure can be viewed at wileyonlinelibrary.com]

50 Plus isocratic pump (Ecom spol. s r.o., Prague, Czech Republic) and took place in the second zone of the extruder. Solid feeding (MCC) took place with a gravimetric twin-screw feeder on a scale platform (K-Tron AG, Niederlenz, Switzerland) in the first zone of the extruder. Continuous cellulose gel strands were extruded at different cellulose concentrations, namely 35 wt% (EX35), 40 wt% (EX40) and 45 wt% (EX45) cellulose (relative to the EmimAc content). The screw speed was 150 rpm with a barrel temperature profile of 20–60–60–80–90 (°C). The screw configuration was divided into a conveying zone, where also the liquid feed took place, a kneading block zone and a compression zone with a reverse conveying element. The extrudates were pelletized using a CSG 171 T strand pelletizer (Dr. Collin GmbH, Ebersberg, Germany). Approximately, 500 gram pellets per gel sample were stored in a polyethylene bag at room temperature for 2 weeks before the next compounding step.

2.2.2 | PLA/cellulose gel compounding

Blends with PLA with a target concentration of PLA/cellulose = 1:1 were compounded with EX35 (compound C35), EX40 (compound C40) and EX45 (compound C45) cellulose gels at 100 rpm in a co-rotating twin screw extruder ZK 27 T × 24 D (Dr. Collin GmbH, Ebersberg, Germany) with length to diameter ratio of 24. Both cellulose gel and PLA granules were predried at 60°C and 40°C, respectively, and manually mixed with their respective weight contents. The seven heating zones varied depending on the compound, but each started at room temperature at the pellet feeder. Ambient degassing was performed in zones 4 and 5 to eliminate evaporating moisture and DMSO. Table 1 shows the applied blend concentrations and extrusion parameters. The screw configuration was composed of alternating conveying, kneading and compression elements as shown in the supporting information (Figure S2). Due to the usual variations in material dosage and ratios when mixing two different solids, as well as the relatively low throughput,

the compounding parameters fluctuate around a certain optimum. Therefore, the averaged samples were selected only within the ranges of melt temperature and die pressure given in Table 1.

The different compositions should show the influence of the cellulose concentration in the cellulose gel on the final blend. Thus, it can be evaluated how high the cellulose concentration may be to still achieve an efficient blend with PLA resulting in a single phase blend. Based on the rheological measurements of the gels and PLA, different temperatures were applied to determine if efficient mixing is possible at temperatures lower than the expected softening points of the cellulose gels due to the higher shear in the compounder.

For comparison, pure PLA LX930 and a PLA/MCC microcomposite (1:1) were also compounded at 170°C.

2.2.3 | Film forming and extraction

To investigate thermomechanical deformability of the blends, plates were prepared using a heatable hydraulic press (Perkin Elmer, Shelton, CT, USA) at a temperature of 150°C for 2 min with a load of 2 tons. The films were cut into strips, and the EmimAc/DMSO were extracted from the film strips with ethanol in a soxhlet apparatus for at least 12 h prior to drying in a vacuum cabinet at 90°C and 40 mbar. For comparison, pure PLA and the PLA/MCC composite were treated the same way. Final film thicknesses ranged from 130 to 170 μm depending on the sample.

2.3 | Analytics

2.3.1 | Rheological analysis

Rheological behavior of the cellulose gels and PLA were examined using a closed cavity rheometer RPA elite (TA Instruments, New Castle, DE, USA). Time sweeps ($T = 150^{\circ}\text{C}$) and strain sweeps were performed prior to temperature and frequency sweeps to ensure thermal

TABLE 1 Applied concentrations and extrusion parameters of PLA/cellulose gel blends

Sample	Mass temperature (°C)	Die pressure (bar)	Cellulose concentration in gel rel. to IL (wt%)	Cellulose gel: PLA ratio (wt/wt)	EmimAc: PLA ratio (wt/wt)	EmimAc: PLA ratio (mol/mol)	Cellulose: PLA ratio (wt/wt)
C35_130°C	131–134	13–21	35	3.08/1 (~9/3)	~1.83/1	~0.78/1	1/1
C35_150°C	151–155	10–16					
C40_130°C	130–135	11–16	40	2.67/1 (~8/3)	~1.48/1	~0.63/1	1/1
C40_150°C	147–152	10–12					
C45_150°C	145–152	11–14	45	2.35/1 (~7/3)	~1.20/1	~0.51/1	1/1
C45_170°C	162–171	5–10					

stability and determine the linear viscoelastic range, respectively. About 5–10 g of the gel sample was placed between two polyamide films and loaded between the two cones in the apparatus, where the sample was pressed at 150°C. Temperature sweeps from 50 to 175°C were performed at constant angular frequency $\omega = 1$ Hz, a strain $\gamma = 1\%$ and a heating rate of 20 K min⁻¹. Frequency sweeps from 0.1–50 Hz were performed at constant strain $\gamma = 1\%$ and temperature $T = 150^\circ\text{C}$.

2.3.2 | Thermal analysis

Thermal analysis of the films by means of differential scanning calorimetry was performed on a Mettler Toledo DSC3+ (Gießen, Germany) and the corresponding evaluation software STARe Version 16.20. The first heating run from 25°C to 120°C, followed by 10 min at 120°C, was used to eliminate residual moisture. After cooling to 0°C, the second heating run was performed to 450°C with a heating/cooling rate of 15 K·min⁻¹. A Linseis STA PT 1600 (Selb, Germany) was used for simultaneous thermogravimetric analysis (TGA) and differential thermal analysis (DTA). Samples were heated from room temperature to 600°C with a heating rate of 15 K·min⁻¹ under nitrogen atmosphere. Sample weights for thermal analysis ranged from 10 to 15 mg.

2.3.3 | Mechanical testing

Mechanical properties of the films were determined using a tensile testing machine Z005 (Allround Line) of Zwick GmbH & Co. KG (Ulm, Germany). Tests were performed with a clamping length of 25 mm at a test speed of 200 mm min⁻¹ with a load shut-off at 95%. Minimum five replicates were tested for each sample, with the exception of C45_150°C, where only two determinations were possible due to the extreme brittleness of the sample, which led to material breakage during preparation

and measurement. OriginPro Version 2018b (Origin Lab Co., Northampton, MA, USA) was used for statistical analysis. A one-way ANOVA was performed. Homogeneity of variances was checked with Brown-Forsythe test. If the effect was significant, we compared multiple means with a post-hoc Tukey test ($p < 0.05$).

2.3.4 | Scanning electron microscopy

Film morphology was examined by scanning electron microscopy (SEM). Pieces of the pressed and extracted films were cryo-fractured to investigate the fracture surface. Cryo-fracturing creates coarse surfaces, prohibiting differentiation between the constituent phases. A complicating factor is that the blend partners are quite similar in their chemical composition and therefore no material differences can be detected on the basis of an SEM image. To determine the blend morphology in this work, one fracture side was treated with HFIP to etch its surface by partial dissolution of PLA. Etched samples were air-dried for a minimum of 48 h to evaporate residual HFIP and sputtered with gold. Prepared samples were examined with a JEOL 7200F scanning electron microscope with a lower electron detector (JEOL, Freising, Germany). Images were taken at an accelerating voltage of 3.0 kV.

2.3.5 | Infrared spectroscopy

FTIR spectra of the films were recorded on a Frontier™ FTIR spectrometer L1280034 using the Spectrum IR software, version 10.6.1, both supplied by Perkin Elmer (Shelton, CT, USA). Measurements were performed at an ambient temperature and pressure. An attenuated total reflectance device was used (Golden Gate™, Specac Ltd., Oprington, UK). A constant contact pressure was achieved by tightening the securing screw with a ratchet limited to a torque of 30 cNm. A total of 16 scans were

recorded within a wavenumber range from 4000 to 600 cm^{-1} with a resolution of 4 cm^{-1} .

2.3.6 | Molecular weight determination

Molecular mass distribution of PLA, PLA/MCC composite and the blends was determined via size exclusion chromatography (SEC) using a Dionex System with HFIP and 0.02 mol L^{-1} trifluoroacetic acid as solvent. A DIONEX Ultimate 3000 injector was used, and the flow rate was fixed to 1 ml min^{-1} (HPLC gradient pump Gynkotek M480). Detection was performed with a refractive index detector Gynkotek SE-61. PSS-PFG columns, tempered to 40°C, were used (PSS, Mainz, Germany: 7 μm , 300 \times 8 mm). Samples were dissolved in HFIP with a concentration of 5000 $\mu\text{g ml}^{-1}$ and filtered with a 0.20 μm PTFE membrane. For the blends, samples were milled with an Ultra Centrifugal Mill ZM 200 (Retsch GmbH, Haan, Germany) and extracted in HFIP for 48 h at room temperature to be able to extract as much PLA as possible. An amount of 40 μl was injected (DIONEX ASI-100). A narrow molecular weight distribution PMMA standard (PSS Mainz, Germany) was used as calibration. The curves were examined with the WinGPC[®]UniChrom (Version 8.1) Software (PSS, Mainz, Germany).

Cellulose degradation during extrusion and storage was exemplarily determined with EX40. The gel was precipitated, soxhlet-extracted with ethanol for at least 12 h to remove EmimAc/DMSO, dried in a vacuum cabinet at 90°C and 40 mbar and grinded with an Ultra Centrifugal Mill ZM 200 (Retsch GmbH, Haan, Germany). The DP was calculated on the basis of intrinsic viscosities following ISO 5351 as well as Kes and Christensen.²⁶

3 | RESULTS AND DISCUSSION

3.1 | Cellulose gel

3.1.1 | Cellulose gel extrusion

Cellulose gels EX35, EX40 and EX45 with high contents of MCC were produced in a continuous extrusion process with EmimAc, chosen based on its high dissolution capacity for cellulose,²⁷ and DMSO. The addition of co-solvent was necessary to lower the solvent viscosity, enabling a stable liquid feed and wetting of the MCC. Since there must be sufficient solidification when the gel strand cools, however, the concentration of the co-solvent was set at 20 vol% after preliminary tests. The gel extrusion step is crucial to increase the availability of the cellulose molecular chains prior the following mixing steps with PLA. Although for dissolution (characterized by

solvent diffusion and chain entanglement) maximum cellulose concentrations in the EmimAc/DMSO system were assumed to be around 25–27 wt%,²⁸ chain availability is also possible at higher ratios based on plasticization and swelling of the polymer.²⁹ However, this clearly depends on the transport processes of the solvent, which are in our case also determined by extrusion parameters such as shear and temperature. Based on known interactions between EmimAc and cellulose,³⁰ extrusion temperatures were kept <100°C to avoid undesired degradation. Still, the DP of the cellulose gels after storage prior to the next compounding step was 270, which correlated to a decrease of ~13% compared to the untreated MCC powder (DP = 310).

3.1.2 | Optical properties

Extruded gels showed inclusion of gas bubbles, which are expected to originate from residual water that could not be removed during predrying or was re-adsorbed during processing. Therefore, some prepared strands still looked opaque after cooling down to room temperature, although transparency was apparent when exiting the die. Strands were coherent at 35 and 40 wt% cellulose. At 45 wt%, the extruded strand broke off at regular intervals and small Microcrystalline cellulose particles were still visible (Figure S1a–c). Therefore, at this cellulose concentration only partial cellulose dissolution or swelling was expected.

3.1.3 | Rheological properties

Cellulose gel strands were granulated and viscoelastic properties were determined using a closed cavity rheometer. Based on the following compounding step, viscosities at certain temperatures and shear rates were of certain interest, since a flow behavior close to that of the PLA was desired for efficient mixing at extrusion conditions.

Temperature sweeps for the extruded gels (Figure 2a) showed solid-like behavior ($G' > G''$) over a wide temperature range for all samples. Unfortunately, the expected cross-over or gel point lies below the resolution limit of the device used. Still, the gel point for EX35 and EX40 are expected to be around 150°C and 170°C, respectively. For the PLA, measurements show a glass transition around 60°C and a flow point at 126°C, which is in line with the manufacturer's data. All gels show a softening with increasing temperature, which can be deduced from the decreasing difference between G' and G'' .

However, only very low shear was applied for the temperature sweeps. To investigate shear dependence, a frequency sweep was performed at 150°C (Figure 2b). This temperature was chosen as low as possible to

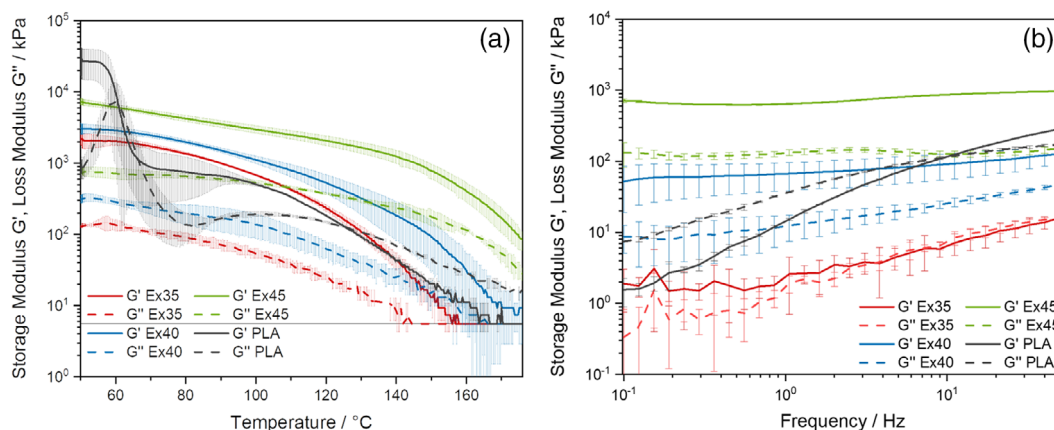


FIGURE 2 (a) Temperature sweep and (b) frequency sweep at 150°C of the cellulose gels EX35 (red), EX40 (blue) and EX45 (green) and PLA LX930 (black) showing storage modulus G' (solid line) and loss modulus G'' (dashed line). The horizontal line depicts the resolution limit of the device during temperature sweep [Color figure can be viewed at wileyonlinelibrary.com]

prevent decomposition, but as high as necessary to allow the gels and the PLA to flow.

As already expected from the temperature sweep, EX35 has its flow point around 150°C, leading to fluctuations between G' and G'' . For both other samples, a maximum frequency of 50 Hz equivalent to a shear rate of 3.068 s^{-1} still represents too little shear to induce flowing. We estimate the average shear rate during our extrusion process to be about 100 s^{-1} ,³¹ which makes flowing of the cellulose gels likely also below 150°C.

To be able to estimate the flow behavior at such high shear rates, flow curves can usually be modeled based on the Cox–Merz rule,³² stating that the complex dynamic viscosity as a function of frequency is consistent with the shear viscosity as a function of shear rate in the non-Newtonian flow regime. However, this empirical rule is only applicable in the absence of energetic interactions (e.g. hydrogen bonding, dipole–dipole interactions),³³ leading to high deviations for polysaccharide gels.³⁴ Therefore, a prediction for the apparent viscosities extrusion temperature and shear rates was not possible based on the performed oscillatory tests.

Since EX40 and EX45 are not actually flowing within the linear viscoelastic range (LVE range) at the applied shear and temperature, it is also not practicable to present the viscosity curves.³⁵ However, to be able to compare all samples and to roughly estimate the flow behavior of the different materials, flow curves of all samples are shown in Figure 3. Both the temperature and frequency sweep show that the viscosity of EX35 is far below the PLA melt, which could lead to difficulties in mixing. Although not flowing, EX40 shows complex viscosities closest to the PLA around and above the 150°C, while EX45 always displays a higher complex viscosity.

3.2 | Cellulose gel/PLA blends and film forming

Preliminary trials using different amorphous and semi-crystalline PLA grades showed that apparent viscosities of the gels and PLA melt should match within the extrusion process to enable efficient mixing (exemplary pictures see Figure S1d and e). Since both components need to flow, temperatures of minimum 130°C (flow point of PLA) had to be applied. However, higher temperatures results in unwanted degradation reactions, therefore, temperatures were limited to 170°C. Blend samples at two different processing temperatures were produced with each cellulose gel. Sample labelling and description can be found in Table 1 in the experimental section.

Already optically visible, higher temperatures led to higher coloring and darkening of the samples (Figure S3). For the highest applied temperatures of 170°C, dark brown and sticky samples were obtained. Imidazole-based ILs are temperature-sensitive and tend to form high-boiling impurities like chromophores and reactive by-products,³⁶ leading to yellow-to-brown coloring²⁰ and also possible degradation of the cellulose^{37,38} as well as degradation of the PLA,³⁹ which will be discussed later. Primarily based on the solvent content, blends showed good thermoplastic behavior and were subsequently hot-pressed to films. Before further characterization, films and were soxhlet-extracted with ethanol for at least 12 h to guarantee sufficient IL and DMSO removal from the samples. This is an important step to be able to discuss the properties of binary PLA/cellulose mixtures, since otherwise the influence of the residual solvent would have to be taken into account.²⁴

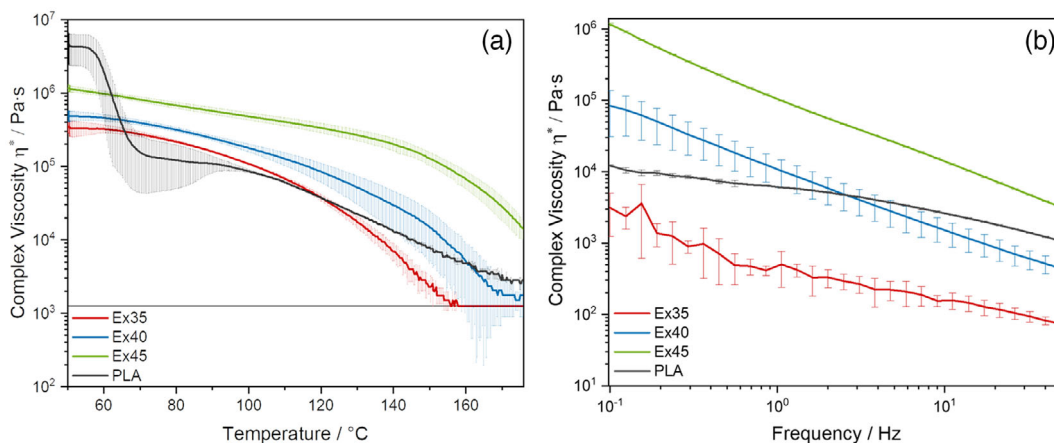


FIGURE 3 Flow curves from (a) temperature sweep and (b) frequency sweep at 150°C of the cellulose gels EX35 (red), EX40 (blue) and EX45 (green) and PLA LX930 (black). The horizontal line depicts the resolution limit of the device during temperature sweep [Color figure can be viewed at wileyonlinelibrary.com]

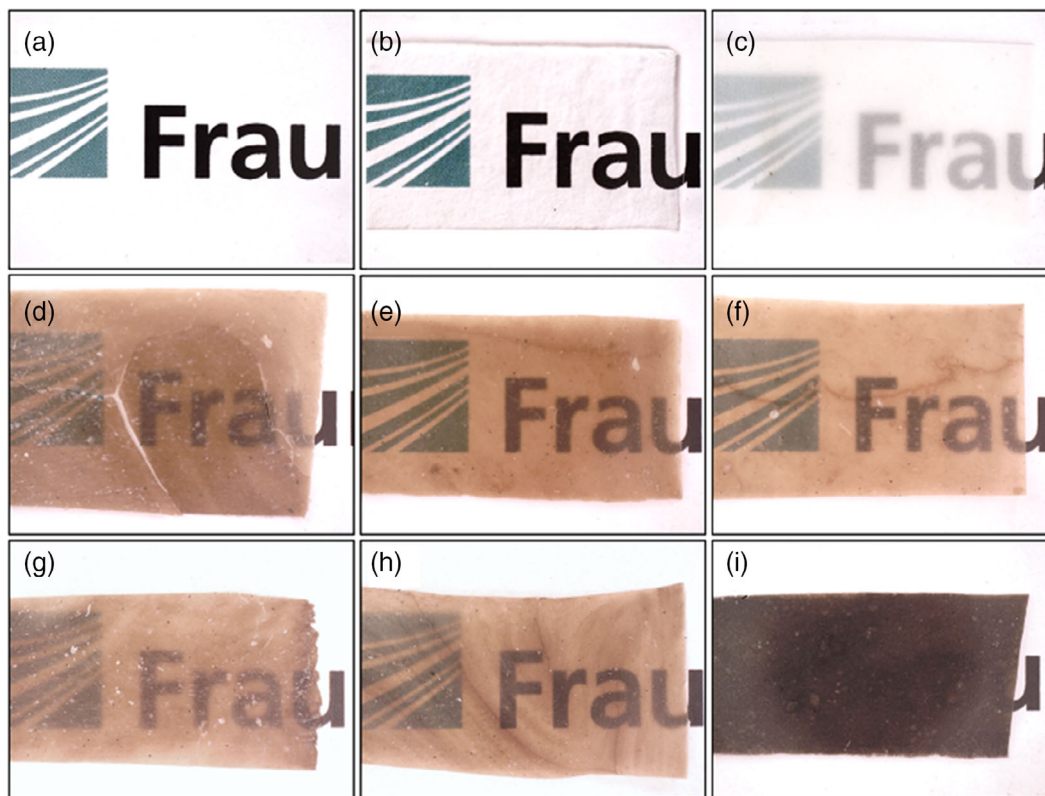


FIGURE 4 Transparency of blend films and references; (a) no film, (b) PLA, (c) PLA/MCC composite, (d) C35_130°C, (e) C40_130°C, (f) C45_150°C, (g) C35_150°C, (h) C40_150°C, and (i) C45_170°C [Color figure can be viewed at wileyonlinelibrary.com]

3.3 | Material properties of extracted blends

3.3.1 | Optical properties

Test strips were mainly transparent but showed a dark color most probably originating from degradation

products of the ionic liquid. Both the C35 and C45 samples showed macroscopically visible particle inclusions and were less flexible. The PLA/MCC microcomposite was more opaque at comparable film thicknesses around 160 μm .

The strong discoloration can be attributed to the formation of high-boiling impurities such as chromophores

in the ionic liquid during processing at higher temperatures.³⁶ Especially in EmimAc, side reactions occur at the C2-atom of imidazolium, with the formation of reactive carbenes.^{36,37} As a function of temperature, the intensity of discoloration increased with extrusion temperature, resulting in dark brown samples at extrusion temperatures of 170°C (Figure 4i).

Blend morphology was examined by SEM using cryo-fractured solvent-etched films (to remove the PLA component). Figure 5 shows the unetched and etched cross-sections of the blends, as well as a PLA/MCC microcomposite and the pure PLA for comparison.

All untreated blends contained small impurities that were most likely undissolved cellulose particles (marked with red circles). However, the size of these inclusions varied among the individual blends. Compared to the PLA/MCC microcomposite (Figure 5g) with particle sizes around 20 µm, cellulose inclusions of about 10 µm (C45, C35) or 2–4 µm (C40) were found. Etched samples showed a smoother surface, but with many cracks. The cellulosic inclusions remained after etching. It is assumed that the cracks originate from swelling of the samples during solvent treatment. When analyzed under high vacuum, the remaining solvent evaporates quickly, leaving the cracked surface.

Based on the limited solubility, high cellulose loads during gel extrusion prevented complete dissolution of the cellulose. Still, due to cellulose swelling, most of the cellulose molecular chains are easily available for further processing, as already investigated during extrusion of lignocellulosic biomass with EmimAc/DMSO.⁴⁰ As expected, crystallinity decreased with an increasing processing temperature and residence time, the latter caused by lower screw speeds.⁴⁰ In our samples, increasing processing temperature also led to a slightly better homogeneity regarding inclusions and general surface smoothness, mainly visible for the C40 samples (Figure S4).

3.3.2 | Structural and thermal properties

Former studies with two-phased composites already revealed that PLA and cellulose interact via hydrogen bonding, mainly concluded from the intensity and shifting of the carbonyl peak.^{41,42} All blends C35, C40, and C45 showed a mixed spectrum with typical bands that can be assigned to both PLA and cellulose (Figure 6). No differences were found between the processing temperatures of the respective blends.

The carbonyl group is one of the most important functional groups involved in the hydrogen bonding of PLA. The band associated with C=O stretching was

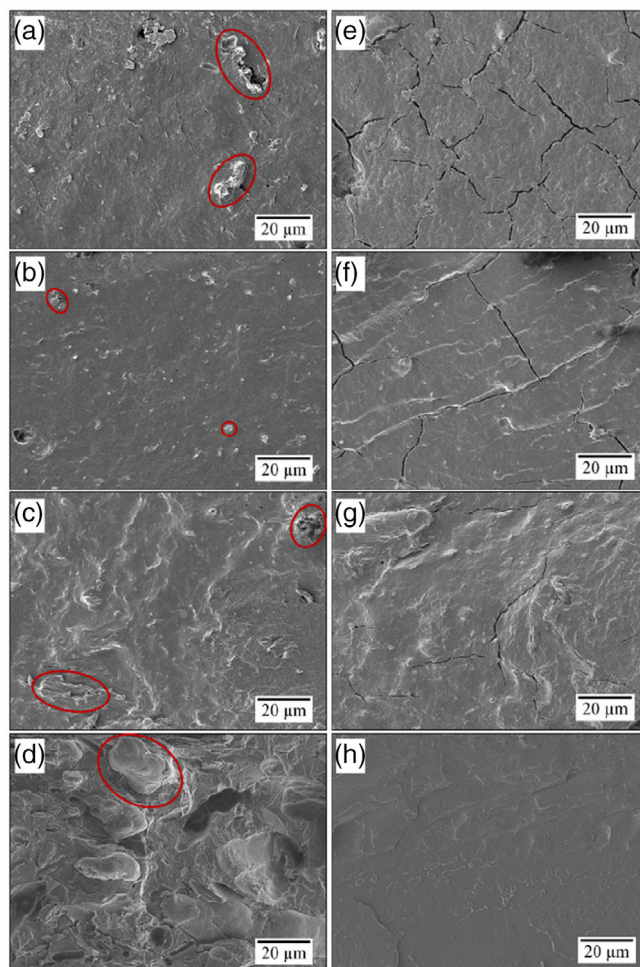


FIGURE 5 SEM images of cryo-fractured cross sections of PLA/cellulose blend films (a) C35_150°C, (b) C40_150°C and (c) C45_170°C and their etched counterparts (e) C35_150°C, (f) C40_150°C, and (g) C45_170°C; PLA/MCC microcomposite film (d) and PLA film (h) [Color figure can be viewed at wileyonlinelibrary.com]

1746 cm⁻¹ for pure PLA and the composite, but shifted to 1736 ± 1 cm⁻¹ for all blends (except C40_130°C). Assuming that efficient mixing allows the formation of hydrogen bonds between the C=O group and the cellulose, the results indicate that interactions between PLA and cellulose can occur down to the molecular level. However, at C40_130°C, the intermixing was not efficient enough to allow homogeneous distribution of the components. We assume that the processing temperature was too low to ensure sufficient flow of the cellulose gel EX40.

Interestingly, new absorption peaks occurred at 3692, 3619, and 796 cm⁻¹. Sharp peaks in the region between 3670 and 3550 cm⁻¹ are usually assigned either to certain inorganic substances and minerals, where they are indicative of a 'free' OH-group either on the surface or within

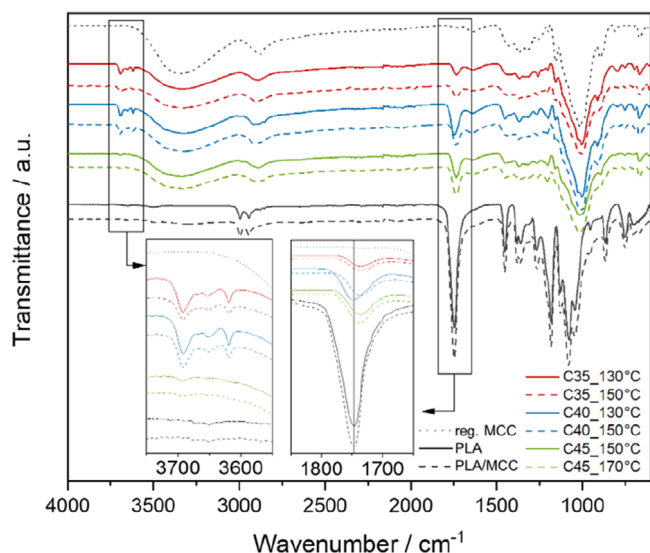


FIGURE 6 FTIR spectra of regenerated cellulose (gray pointed), C35 compounded at 130°C (red solid) and 150°C (red dashed); C40 compounded at 130°C (blue solid) and 150°C (blue dashed), C45 compounded at 150°C (green solid) and 170°C (green dashed), extruded PLA (black solid) and a PLA/MCC composite (black dashed) [Color figure can be viewed at wileyonlinelibrary.com]

a crystal lattice, or to alcohols or phenols with a sterically hindered hydroxyl group.⁴³

The latter may be explained by a higher amount of energy needed to interact with the mid-infrared radiation, since the fundamental vibrations are impeded. Possible structures that could be presented in the blends are reaction products from the cellulose itself or sugars derived from cellulose degradation reacting with the imidazolium. Comparable reactions of butylmethylimidazolium with glucopyranose and cellulose at its reducing end, respectively, have been described by Ebner et al.³⁷ The peaks were most pronounced in the C35 and C40 samples, which would support the described reaction due to their higher IL content. The other small peak at 796 cm^{-1} may be assigned to the C=O from PLA oligomers,⁴⁴ which also fits the DSC results shown later.

Degradation of the PLA was investigated using relative SEC measurements to determine the molecular weight distribution (Figure 7) and calculated molecular weight averages (Table S1). Please note that for SEC measurement of the PLA content in the blend, the entire PLA fraction must be dissolved or extracted from the blend. Since most PLA chains, which form a dense, amorphous network with the cellulose, are presumably trapped between the rigid cellulose chains, even ground samples are likely to have non-extractable PLA chains that are not accounted for in the analysis presented. Mass balancing (after grinding and extraction in HFIP for 5 d)

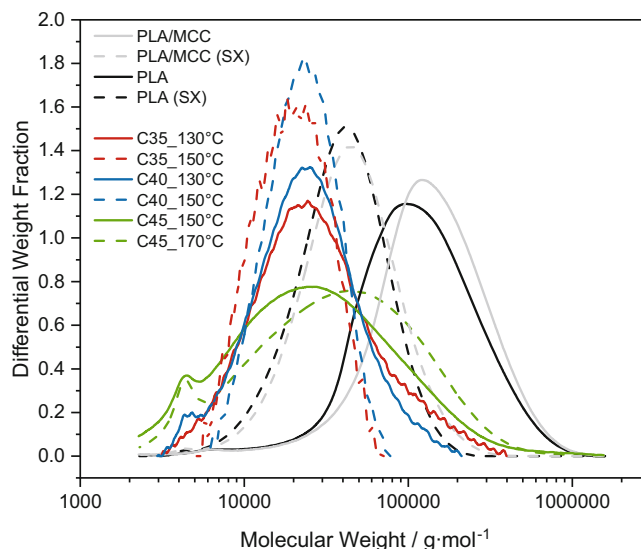


FIGURE 7 Molecular mass distribution of PLA from soxhlet extracted blends C35 compounded at 130°C (red solid) and 150°C (red dashed); C40 compounded at 130°C (blue solid) and 150°C (blue dashed), C45 compounded at 150°C (green solid) and 170°C (green dashed), extruded PLA (black solid) and a PLA/MCC composite (gray solid) and soxhlet treated PLA (black dashed) and PLA/MCC composite (gray dashed) [Color figure can be viewed at wileyonlinelibrary.com]

showed that on average only 10 wt% PLA was extracted from the blends with HFIP, while the residue showed the similar IR to the input materials (no change in carbonyl band). These results, on the one hand, make the SEC analytics of the blend unrepresentative, but on the other hand, confirm the largely homogeneous morphology of the blends. Although this means that absolute values for the blends are strongly erroneous, a comparison within the blend samples still seems reasonable.

Polylactic acid as a polyester is sensitive to hydrolysis and thermal degradation.^{45,46} Two different factors are considered within our process: (a) extrusion and storage in the presence of basic IL at different temperatures and (b) soxhlet extraction with ethanol. Regarding the latter, even with small amounts of residual water, PLA hydrolytic degradation occurs in the environment of ethanol.⁴⁷ During soxhlet extraction, elevated temperatures are applied, which might lead to an intensification of the reaction. For the pure PLA and the PLA/MCC composite samples, soxhlet extraction highly decreased their M_w from approximately 160 $\text{kg}\cdot\text{mol}^{-1}$ to 50 $\text{kg}\cdot\text{mol}^{-1}$ with a slightly narrower distribution.

The gel blends and the extracted blends were measured at the same time, that is, the gels had already been stored for several weeks at ambient conditions. Comparing the gel blends to the extracted blends, it can be assumed that the entire PLA fraction is dissolved. All gel

samples showed substantial degradation of PLA down to M_w between 23 and 50 kg·mol⁻¹ (Figure S5). Therefore, it may be assumed that storage time was accompanied by further degradation (also visible with repeated measurements between 4 weeks, data not shown). For the extracted samples showing similar M_w , we suggest that the soxhlet treatment is not the main factor for PLA degradation in the blends. We suppose that rather degradation reactions caused by the IL are dominant.

Depending on temperature and exposure time, the basic imidazolium acetate can cause a strong decomposition of PLA. The increase of the PLA degradation correlates with the increase of the IL concentration. The highest degradation rate was found between 130°C and 150°C for 1-octyl-3-methylimidazolium acetate.³⁹ In EmimAc, PLA was found to degrade up to almost 50% at a molar ratio of 1:1 (PLA:IL) at 150°C for 1 h.³⁹ However, less IL is present in our extruded samples (molar ratio ~ 1.3–1.9:1). Moreover, most of the IL is not freely available because of the interaction with cellulose, and the reaction time in the extruder is much shorter, about 10 min. Nevertheless, the M_w of the extracted blends ranged from 24 to 62 kg·mol⁻¹. For high EmimAc concentrations (C35, C40), higher extrusion temperatures lead to more degradation. This effect was not visible for the C45 samples. These samples showed in addition to the broad peak a small peak in the range around 4.5 kg·mol⁻¹.

DSC thermograms of the C35–45 samples showed no typical glass transition as expected for PLA (Figure 8). We previously discussed the absence of its T_g in solution-blended samples.²⁴ In a polymer blend with separate phases of the blend partners, two separate glass transitions are present. In a miscible system, only one transition can be detected, which lies between the transitions of the individual components, depending on the concentration of the polymers.⁴⁸ Very low degrees of phase separation, on the other hand, have been associated with a very broad T_g value between those of the pure components,⁴⁹ which may not be clearly determined by DSC. Based on the thermograms and our previous results, we assume an interpenetrating polymer network of PLA and cellulose with a small share of microphase-separated amorphous regions.

Interestingly, an endothermic thermal event around 108°C occurred for the C35 (130 and 150°C) and C40 (130°C) samples. Since this was determined for the second heating run and this event was already visible in the cooling run, it can be attributed to melting/crystallization of a polymer structure rather than water or solvent evaporation. One possible explanation could be the crystallization of PLA oligomers. Although we used an amorphous grade with a D-isomer content of 8%, which hinders crystallization of PLLA chains, PLA degradation

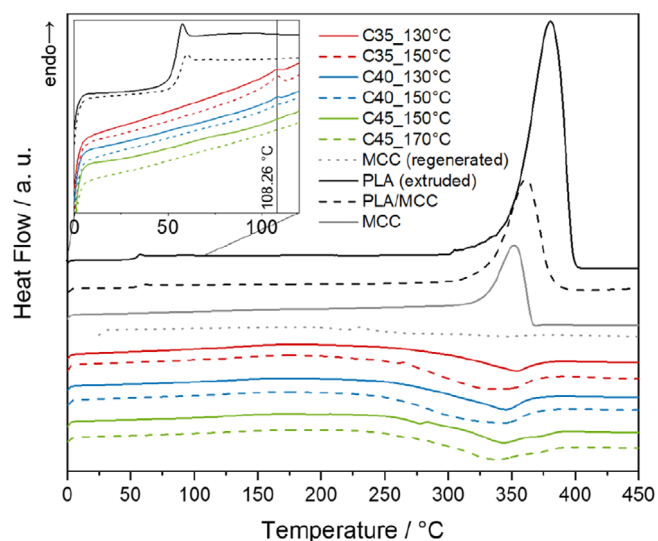


FIGURE 8 DSC thermograms of regenerated cellulose (gray pointed), microcrystalline cellulose (MCC, gray), C35 compounded at 130°C (red solid) and 150°C (red dashed); C40 compounded at 130°C (blue solid) and 150°C (blue dashed), C45 compounded at 150°C (green solid) and 170°C (green dashed), extruded PLA (black solid) and a PLA/MCC composite (black dashed) from the second heating run [Color figure can be viewed at wileyonlinelibrary.com]

might have resulted in oligomers with relatively few or no D-isomers. In addition, swelling of the samples during soxhlet extraction may have promoted rearrangement of the polymer chains and subsequent crystallization.^{47,50} Comparable PLA oligomers with DP < 10 showed melting points in the same temperature range around 110°C.^{44,51}

The thermal stability of the blends and material components was investigated by means of TGA coupled with DTA (Figure 9). Usually, weight reduction occurs first due to the loss of contained moisture, followed by massive weight reduction due to thermal degradation. Cellulose, based on its chemical composition, can absorb much more water from the atmosphere than PLA,^{52–56} therefore, the moisture loss of PLA and its composite was the lowest. Both showed an onset of degradation at ~316°C, while the degradation of MCC started around 304°C. In general, regenerated cellulose shows lower degradation temperatures than native cellulose^{57–59} with an onset of ~218°C, also due to its low crystallinity from ethanol precipitation.⁶⁰ For the blends, thermal stability increased compared to regenerated cellulose, while it decreased compared to MCC, PLA, and their composite.

For regenerated cellulose and blends, the degradation is clearly divided into two main steps with a plateau in between. The first step (I) is accompanied by a broad endothermic event, presumably due to breakage of long

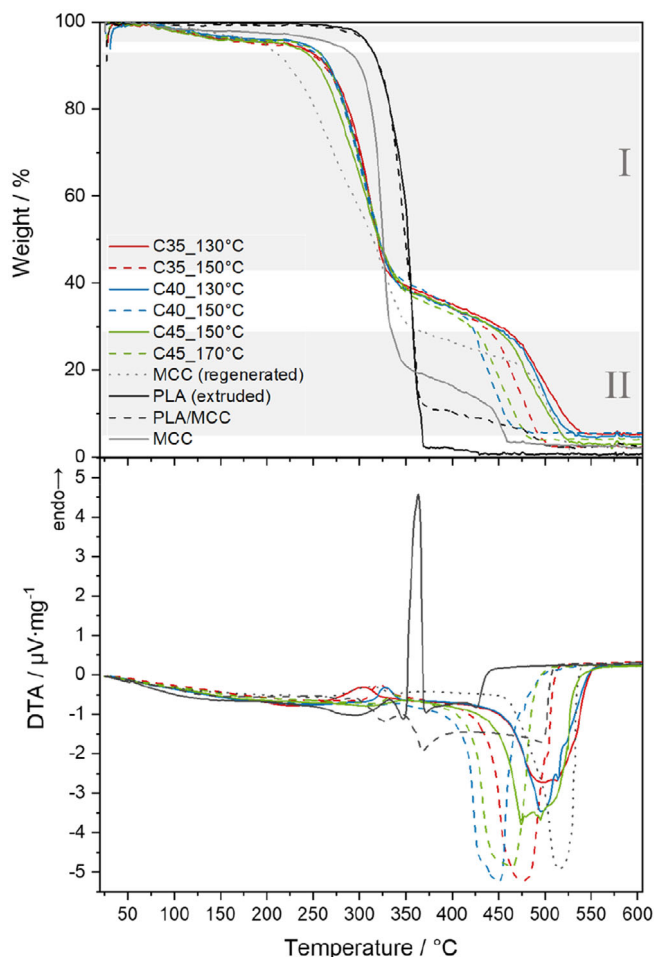


FIGURE 9 Thermogravimetric analysis and DTA thermograms of regenerated cellulose (gray pointed), MCC (gray), C35 compounded at 130°C (red solid) and 150°C (red dashed); C40 compounded at 130°C (blue solid) and 150°C (blue dashed), C45 compounded at 150°C (green solid) and 170°C (green dashed), extruded PLA (black solid) and a PLA/MCC composite (black dashed) [Color figure can be viewed at wileyonlinelibrary.com]

polysaccharide chains, as was already suggested for starch materials.⁶¹ The second degradation step (II) at temperatures of 420–540°C is caused by pyranose ring opening of the glucose units, as was previously proposed for starch and cellulose acetate, although the steps were not as pronounced as in our samples.^{61,62}

In this second step, differences between the blends become visible with regard to their processing temperatures. While lower extrusion temperatures resulted in higher stability, all blends compounded at higher temperatures (dashed lines) showed faster degradation. Since cellulose degradation already occurred during extrusion temperatures and is a function of temperature,^{30,63} the glucose concentration increases much faster, and therefore pyrolysis starts earlier. Additionally, the pyrolysis

temperature depends on the crystallinity of a substance.⁵⁹ Since the blends are expected to be completely amorphous in the mixed areas,²⁴ the second steps start way before the regenerated cellulose.

PLA and its composite shows highest thermal stability, with a degradation onset at ~316 °C, accompanied by a large endothermic peak and severe weight loss due to lactic acid evaporation. Although all blends are composed of 50 wt% PLA, no such endothermic peak was detected during DSC measurement. Therefore, the evaporation of lactic acid could be much slower than that of the PLA-only samples because the PLA chains are entrapped in the cellulose network.

3.3.3 | Mechanical properties of pressed films

Most of the extracted blends were extremely brittle. As a result, the C35 specimens could not be cut to the required dimensions, and other specimens broke during specimen preparation or specimen clamping, resulting in a reduced number of replicates (C45_150°C).

Compared to a microcomposite, a homogeneous polymer blend is expected to have higher mechanical performance in terms of tensile strength and elongation due to better load transfer between the compatible phases. In terms of modulus of elasticity, which is measured in the elastic range at very low loads, load transfer is of less importance; rather, the stiffness of the individual phases determines the stiffness of the material. Therefore, a microcomposite reinforced with crystalline cellulose is expected to have a higher modulus than the amorphous blend. Regarding the modulus, our samples showed the expected behavior (Figure 10). No significant differences were found between the blends, and both the blends and the composite exhibited higher modulus than the pure PLA (ANOVA: $F_{6,28} = 13.66$; $p = 3.36 \cdot 10^{-7}$, and $R^2 = 0.74$). Reinforced PLA with MCC exhibited higher moduli with increasing MCC content.⁶⁴ Absolute values for the Young's modulus of injection molded PLA and a PLA/MCC (1:1) microcomposite of ~2500 MPa are comparable to our data.⁶⁵ Although not significant for all blend samples, the microcomposite in this study showed slightly higher stiffness of 42 MPa⁶⁵ than our samples, probably due to their higher crystallinity the MCC and PLA type used.

For the other two mechanical key values, the measurements deviated from expectations and showed significantly lower or the same values as the composite (tensile strength: $F_{6,28} = 35.93$, $p = 6.61 \cdot 10^{-12}$, and $R^2 = 0.89$; elongation at break: $F_{6,28} = 87.66$, $p = 7.73 \cdot 10^{-17}$, and $R^2 = 0.95$). Within the blends, tensile strength and

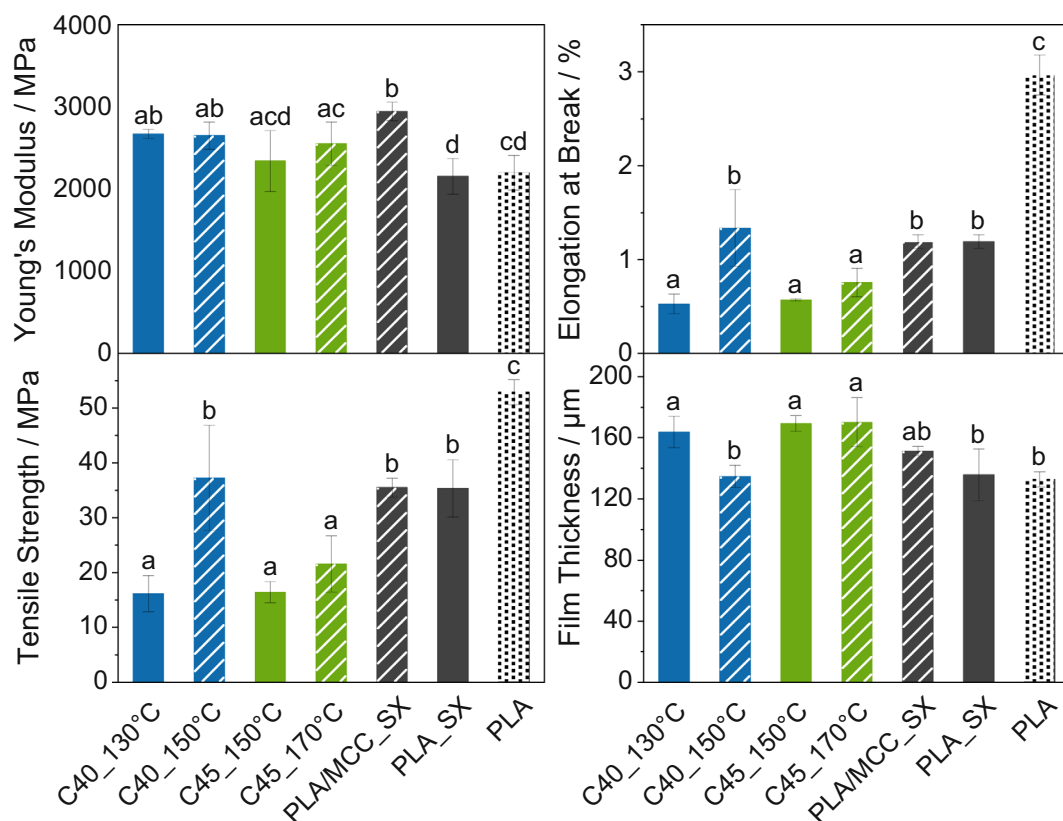


FIGURE 10 Young's modulus, tensile strength, elongation at break and film thickness of tested samples. Different letters show statistically significant ($p < 0.05$) differences between means [Color figure can be viewed at wileyonlinelibrary.com]

elongation are assumed to increase with increasing degree of mixing or homogeneity of the blend. The highest tensile strength and elongation were found for the C40 extruded at 150 °C, while all other samples had significantly lower values. It should be noted, that elongation values highly depend on the film thickness, which also differed between the samples ($F_{6,28} = 9.81$, $p = 7.70 \cdot 10^{-6}$, and $R^2 = 0.68$). As noted in the SEM analysis, higher temperatures resulted in a more homogeneous blend morphology as they allowed for more efficient mixing (Figure S4). The C40 blends were expected to have the highest compatibility in terms of the flow properties of PLA and the cellulose gel during the rheological tests, resulting in the smoothest morphology and the highest strength and elongation. Not only the comparison within our sample sets, but also with other studies preparing homogeneous PLA/cellulose blends illustrates the significant influence of the blend morphology. Blends of the same PLA/cellulose percentage, prepared via solution-precipitation process with 1-butyl-3-methylimidazolium acetate, showed a tensile strength of only 15 MPa.²¹ Being comparable to blends with lower mixing degrees from our study (C40_130°C, C45_150°C), we assume that no sufficient mixing was achieved by the

other group. This is also evident from DSC data showing crystallization of PLA in the blends.²¹

As mentioned earlier, the homogeneous, nearly single-phase morphology in some of our blends suggests higher mechanical strength but lower stiffness than heterophasic composites of PLA and cellulose. The absence of such significant effects compared to the composite and the original PLA therefore requires an explanation. The absence of such significant effects compared to the composite and the original PLA therefore requires an explanation. The first factor resulting from the molecular weight distribution of PLA is that not only processing with IL but also soxhlet extraction led to degradation reactions of PLA. Especially in elongation and tensile strength, the molecular weight of the polymer has a great influence on the performance, for example, due to the entanglement of the PLA chains, which allows higher elongation. Considering the molecular weight, the strength values of the soxhlet-extracted PLA are comparable to injection-molded samples with M_w of $\sim 50 \text{ kg} \cdot \text{mol}^{-1}$, showing values of $\sim 40 \text{ MPa}$.⁶⁶ On the positive side, the C40 blend has a comparable tensile strength and elongation despite its lower molar mass than the composite. A second factor affecting tensile strength and elongation of the blends

could be the higher levels of impurities. As discussed earlier, processing of imidazolium-based ILs at temperatures above 120°C is associated with degradation processes and the formation of chromophores, which apparently remained in the samples after extraction (Figure 4). Although there is little comparable literature, regenerated cellulosic fibers also showed decreased mechanical properties at higher impurity levels,⁶⁷ such as lower tenacity and elongation at break after repeated dissolution/regeneration cycles with the same ionic liquid.⁶⁸

4 | CONCLUSION AND OUTLOOK

We demonstrated that an efficient blending between PLA and cellulose can be achieved by a continuous extrusion process using only small amounts of solvent as intermediate compatibilizer. Cellulose gels with 40 wt% cellulose showed viscosities comparable to the PLA melt at applied processing temperatures, enabling efficient mixing during compounding. Resulting PLA/cellulose gel blends were thermoformable into films by compression molding. After IL and co-solvent extraction, transparent films showed a homogeneous morphology with only low cellulose particle inclusions, and intense polymer interactions in the main phase were concluded from FTIR and DSC analysis. The cellulose blend from 40 wt% gels compounded at 150°C showed strength and elongation with 37 MPa and 1.34% comparable to a PLA/MCC composite and pure PLA. Based on the blend morphology, however, facilitated load transfer should result in a material with higher strength compared to the multiphase composite. Reasons are found with polymer degradation: the PLA in the blend had a molecular weight of only 24 kg·mol⁻¹, while the composite showed 53 kg·mol⁻¹. Additionally, IL degradation products led to impurities that further decreased strength and elongation. For the PLA degradation, the influence of IL concentration was more obvious than the influence of processing temperature or Soxhlet extraction. Therefore, extrusion temperatures should be as low as possible but as high as needed to ensure flow. Although side reactions can be reduced, for example, by using processing temperatures below 120°C or increasing the initial acidity, they cannot be fully prevented.²⁰ For further investigations, the authors recommend different strategies to prevent severe degradation: (1) change of the IL by choosing a less basic anion and/or changing the cation,^{20,69} (2) inhibition of cellulose degradation in IL, for example, by adding glycerol⁶⁹ or amino acids⁷⁰ (3) reduction in melt viscosity of the PLA with additives such as plasticizers to reduce the processing temperatures.^{71–73}

The importance of reducing such degradation becomes even greater when considering the economics of the process. Ensuring reasonable material costs requires a functioning ionic liquid cycle, including solvent recovery and purification. Although this study focused on the material preparation process itself, the future studies must also address IL recycling, particularly in the context of larger scale processing. Larger batches of material would also help to reduce variations in the extrusion process by aiming for higher throughput and longer process times to stabilize the process parameters. As for the final blend properties, interesting features such as transparency and biodegradability should be further investigated in the future to understand these phenomena fundamentally.

AUTHOR CONTRIBUTIONS

Kerstin Müller: Conceptualization (lead); formal analysis (lead); investigation (lead); methodology (lead); visualization (lead); writing – original draft (lead); writing – review and editing (equal). **Siegfried Fürtauer:** Writing – review and editing (equal). **Markus Schmid:** Writing – review and editing (equal). **Cordt Zollfrank:** Writing – review and editing (equal).

ACKNOWLEDGMENTS

The authors thank their colleagues Weixuan Wang (TUM), Norbert Rodler and Michael Stenger (both IVV) for their support with TGA and extrusion/compounding of the materials. We further thank Andreas Mäurer for his valuable comments on the article. Open Access funding enabled and organized by Projekt DEAL.

DATA AVAILABILITY STATEMENT

The data that support the findings of this study are available in the supplementary material of this article. Any further data are available from the corresponding author upon reasonable request.

ORCID

Kerstin Müller  <https://orcid.org/0000-0002-7737-4911>

REFERENCES

- [1] A. Xu, F. Wang, L. Zhang, X. Xu, Z. Xiao, R. Liu, *J. Appl. Polym. Sci.* **2021**, *138*, 50320.
- [2] N. Mayilswamy, B. Kandasubramanian, *Emergent Materials* **2022**. <https://doi.org/10.1007/s42247-022-00354-2>
- [3] S. Chueter, P. Tantayotai, K. Cheenkachorn, Y.-S. Cheng, A. Tawai, M. Sriariyanun, in *Biodegradable Polymers, Blends and Composites* (Eds: S. Mavinkere Rangappa, J. Parameswaranpillai, S. Siengchin, M. Ramesh), Woodhead Publishing, Duxford **2022**.
- [4] M. S. Andrade, O. H. Ishikawa, R. S. Costa, M. V. S. Seixas, R. C. L. B. Rodrigues, E. A. B. Moura, *Food Packag Shelf Life* **2022**, *31*, 100807.

- [5] X. Wu, Y. Liu, H. Wu, Y. Duan, J. Zhang, *Compos. Sci. Technol.* **2022**, *218*, 109135.
- [6] X. Zhang, X. Wu, D. Gao, K. Xia, *Carbohydr. Polym.* **2012**, *87*, 2470.
- [7] J. Schroeter, F. Felix, *Cellulose* **2005**, *12*, 159.
- [8] Q. Wang, J. Cai, L. Zhang, M. Xu, H. Cheng, C. C. Han, S. Kuga, J. Xiao, R. Xiao, *J. Mater. Chem. A* **2013**, *1*, 6678.
- [9] T. I. A. Gouveia, K. Biernacki, M. C. R. Castro, M. P. Gonçalves, H. K. S. Souza, *Food Hydrocolloids* **2019**, *97*, 105175.
- [10] R. P. Swatloski, S. K. Spear, J. D. Holbrey, R. D. Rogers, *J. Am. Chem. Soc.* **2002**, *124*, 4974.
- [11] C. Hopson, M. M. Villar-Chavero, J. C. Domínguez, M. V. Alonso, M. Oliet, F. Rodriguez, *Carbohydr. Polym.* **2021**, *274*, 118663.
- [12] A. Takada, J.-I. Kadokawa, *Cellulose* **2021**, *29*, 2745.
- [13] A. A. Shamsuri, S. N. A. Md. Jamil, K. Abdan, *Polymers* **2021**, *13*, 2597.
- [14] M. A. Haq, Y. Habu, K. Yamamoto, A. Takada, J.-I. Kadokawa, *Carbohydr. Polym.* **2019**, *223*, 115058.
- [15] S. P. F. Costa, A. M. O. Azevedo, P. C. A. G. Pinto, M. L. M. F. S. Saraiva, *ChemSusChem* **2017**, *10*, 2321.
- [16] H. Baaqel, I. Díaz, V. Tulus, B. Chachuat, G. Guillén-Gosálbez, J. P. Hallett, *Green Chem.* **2020**, *22*, 3132.
- [17] F. Philippi, D. Rauber, K. L. Eliassen, N. Bouscharain, K. Niss, C. W. M. Kay, T. Welton, *Chem. Sci.* **2022**, *13*, 2735.
- [18] N. D. Khupse, A. Kumar, *J. Solution Chem.* **2009**, *38*, 589.
- [19] F. Yang, P. Feng, *Appl. Sci.* **2020**, *10*, 8342.
- [20] M. T. Clough, K. Geyer, P. A. Hunt, S. Son, U. Vagt, T. Welton, *Green Chem.* **2015**, *17*, 231.
- [21] A. Xu, Y. Wang, J. Gao, J. Wang, *Green Chem.* **2019**, *21*, 4449.
- [22] R. S. J. Manley, *In Cellulose Derivatives*, American Chemical Society, Washington, DC **1998**, Ch. 18.
- [23] K. Müller, C. Zollfrank, *Eur. Polym. J.* **2020**, *133*, 109743.
- [24] K. Müller, D. Van Opdenbosch, C. Zollfrank, *Mater. Today Commun.* **2022**, *30*, 103074.
- [25] X. Niu, S. Huan, H. Li, H. Pan, O. J. Rojas, *J. Hazard. Mater.* **2021**, *402*, 124073.
- [26] M. Kes, B. E. Christensen, *J. Chromatogr. A* **2013**, *1281*, 32.
- [27] Y.-R. Liu, K. Thomsen, Y. Nie, S.-J. Zhang, A. S. Meyer, *Green Chem.* **2016**, *18*, 6246.
- [28] K. A. Le, C. Rudaz, T. Budtova, *Carbohydr. Polym.* **2014**, *105*, 237.
- [29] B. A. Miller-Chou, J. L. Koenig, *Prog. Polym. Sci.* **2003**, *28*, 1223.
- [30] S. Dorn, F. Wendler, F. Meister, T. Heinze, *Macromol. Mater. Eng.* **2008**, *293*, 907.
- [31] B. Vergnes, *Polymer* **2021**, *13*, 304.
- [32] W. P. Cox, E. H. Merz, *J. Polym. Sci.* **1958**, *28*, 619.
- [33] W. M. Kulicke, R. S. Porter, *Rheol. Acta* **1980**, *19*, 601.
- [34] C. Seidel, W.-M. Kulicke, C. Heß, B. Hartmann, M. D. Lechner, W. Lazik, *Starch-Stärke* **2001**, *53*, 305.
- [35] T. G. Mezger, *The Rheology Handbook*, Vincentz Network, Hanover, Germany 2012.
- [36] M. Watts, B. Kosan, J. Hammerschmidt, S. Dorn, F. Meister, S. Scholl, *Chem. Ing. Tech.* **2017**, *89*, 1661.
- [37] G. Ebner, S. Schiehser, A. Potthast, T. Rosenau, *Tetrahedron Lett.* **2008**, *49*, 7322.
- [38] E. Ohno, H. Miyafuji, *J. Wood Sci.* **2014**, *60*, 428.
- [39] X.-Y. Li, Q. Zhou, K.-K. Yang, Y.-Z. Wang, *Chem. Pap.* **2014**, *68*, 1375.
- [40] S. Y. Han, C. W. Park, T. Endo, F. Febrianto, N.-H. Kim, S.-H. Lee, *Wood Sci Technol.* **2020**, *54*, 599.
- [41] W. H. Wan Ishak, N. A. Rosli, I. Ahmad, *Sci. Rep.* **2020**, *10*, 11342.
- [42] N. A. Rosli, I. Ahmad, F. H. Anuar, I. Abdullah, *Cellulose* **2019**, *26*, 3205.
- [43] J. Coates, in *Encyclopedia of Analytical Chemistry* (Eds: R. A. Meyers, M. L. McKelvy), John Wiley & Sons, Ltd, New Jersey **2006**.
- [44] J. Ambrosio-Martín, M. J. Fabra, A. Lopez-Rubio, J. M. Lagaron, *J. Mater. Sci.* **2014**, *49*, 2975.
- [45] A. A. Cuadri, J. E. Martín-Alfonso, *Polym. Degrad. Stab.* **2018**, *150*, 37.
- [46] V. Speranza, A. De Meo, R. Pantani, *Polym. Degrad. Stab.* **2014**, *100*, 37.
- [47] F. Iñiguez-Franco, R. Auras, G. Burgess, D. Holmes, X. Fang, M. Rubino, H. Soto-Valdez, *Polymer* **2016**, *99*, 315.
- [48] T. G. Fox, *Bullet. Am. Phys. Soc.* **1956**, *1*, 123.
- [49] L. A. de Graaf, M. Möller, *Polymer* **1995**, *36*, 3451.
- [50] S. Sato, D. Gondo, T. Wada, S. Kanehashi, K. Nagai, *J. Appl. Polym. Sci.* **2013**, *129*, 1607.
- [51] M. R. ten Breteler, J. Feijen, P. J. Dijkstra, F. Signori, *React. Funct. Polym.* **2013**, *73*, 30.
- [52] R. A. Cairncross, S. Ramaswamy, R. O'Connor, *Int. Polym. Process.* **2007**, *22*, 33.
- [53] M. Garg, V. Apostolopoulou-Kalkavoura, M. Linares, T. Kaldéus, E. Malmström, L. Bergström, I. Zozoulenko, *Cellulose* **2021**, *28*, 9007.
- [54] K. Kachrimanis, M. F. Noisternig, U. J. Griesser, S. Malamataris, *Eur. J. Pharm. Biopharm.* **2006**, *64*, 307.
- [55] D. Koo, A. Du, G. R. Palmese, R. A. Cairncross, *Polymer* **2012**, *53*, 1115.
- [56] J. Trifol, D. Plackett, P. Szabo, A. E. Daugaard, M. Giacinti Baschetti, *ACS Omega* **2020**, *5*, 15362.
- [57] N. Muhammad, Z. Man, M. Azmi Bustam Khalil, I. M. Tan, S. Maitra, *Waste Biomass Valoriz.* **2010**, *1*, 315.
- [58] A. Shakeri, M. P. Staiger, *BioResources* **2010**, *5*, 979.
- [59] H. Satani, M. Kuwata, A. Shimizu, *Carbohydr. Res.* **2020**, *494*, 108054.
- [60] X. Tan, L. Chen, X. Li, F. Xie, *Int. J. Biol. Macromol.* **2019**, *124*, 314.
- [61] X. Liu, L. Yu, H. Liu, L. Chen, L. Li, *Cereal Chem.* **2009**, *86*, 383.
- [62] M. Da, C. C. Lucena, A. E. De-Alencar, S. E. Mazzeto, E. S. De, *Polym. Degrad. Stab.* **2003**, *80*, 149.
- [63] J. L. Thomason, J. L. Rudeiros-Fernández, *Polym. Degrad. Stab.* **2021**, *188*, 109594.
- [64] A. P. Mathew, K. Oksman, M. Sain, *J. Appl. Polym. Sci.* **2005**, *97*, 2014.
- [65] U. C. Paul, D. Fragouli, I. S. Bayer, A. Zych, A. Athanassiou, *ACS Appl. Polym. Mater.* **2021**, *3*, 3071.
- [66] G. Perego, G. D. Cella, C. Bastioli, *J. Appl. Polym. Sci.* **1996**, *59*, 37.
- [67] M. Watts, PhD Thesis, Technical University Braunschweig **2019**.
- [68] S. Elsayed, S. Hellsten, C. Guizani, J. Witos, M. Rissanen, A. H. Rantamäki, P. Varis, S. K. Wiedmer, H. Sixta, *ACS Sustain. Chem. Eng.* **2020**, *8*, 14217.

- [69] M. T. Clough, J. A. Griffith, O. Kuzmina, T. Welton, *Green Chem.* **2016**, *18*, 3758.
- [70] J. Yang, X. Lu, X. Yao, Y. Li, Y. Yang, Q. Zhou, S. Zhang, *Green Chem.* **2019**, *21*, 2777.
- [71] H. Ge, F. Yang, Y. Hao, G. Wu, H. Zhang, L. Dong, *J. Appl. Polym. Sci.* **2013**, *127*, 2832.
- [72] D. Xie, Y. Zhao, Y. Li, A. M. LaChance, J. Lai, L. Sun, J. Chen, *Materials* **2019**, *12*, 3519.
- [73] R. N. Darie-Niță, C. Vasile, A. Irimia, R. Lipșa, M. Râpă, *J. Appl. Polym. Sci.* **2015**, *133*, 1332016.

SUPPORTING INFORMATION

Additional supporting information can be found online in the Supporting Information section at the end of this article.

How to cite this article: K. Müller, S. Fürtauer, M. Schmid, C. Zollfrank, *J. Appl. Polym. Sci.* **2022**, *139*(37), e52794. <https://doi.org/10.1002/app.52794>